Swarm and Evolutionary Computation 53 (2020) 100626

Contents lists available at ScienceDirect

Swarm and Evolutionary Computation

journal homepage: www.elsevier.com/locate/swevo

Applying graph-based differential grouping for multiobjective large-scale optimization

Bin Cao [a,b,c], Jianwei Zhao [a,b], Yu Gu [d,e,**], Yingbiao Ling [f,g,*], Xiaoliang Ma [h]

[a] State Key Laboratory of Reliability and Intelligence of Electrical Equipment, Hebei University of Technology, Tianjin 300401, China
[b] School of Artificial Intelligence, Hebei University of Technology, Tianjin 300401, China
[c] Hebei Provincial Key Laboratory of Big Data Calculation, Tianjin 300401, China
[d] Beijing Advanced Innovation Center for Soft Matter Science and Engineering, Beijing University of Chemical Technology, Beijing 100029, China
[e] Department of Chemistry, Institute of Inorganic and Analytical Chemistry, Goethe-University, Frankfurt 60438, Germany
[f] Key Laboratory of Machine Intelligence and Advanced Computing (Sun Yat-sen University), Ministry of Education, Guangzhou 510006, China
[g] School of Data and Computer Science, Sun Yat-sen University, Guangzhou 510006, China
[h] College of Computer Science and Software Engineering, Shenzhen University, Shenzhen 518060, China

ARTICLE INFO

Keywords:
Differential grouping
Graph-based differential grouping
Multiobjective optimization
Large-scale optimization

ABSTRACT

An increasing number of multiobjective large-scale optimization problems (MOLSOPs) are emerging. Optimization based on variable grouping and cooperative coevolution is a good way to address MOLSOPs, but few attempts have been made to decompose the variables in MOLSOPs. In this paper, we propose multiobjective graph-based differential grouping with shift (mogDG-shift) to decompose the large number of variables in an MOLSOP. We analyze the variable properties, then detect the interactions among variables, and finally group the variables based on their properties and interactions. We modify the decision variable analyses (DVA) in the multiobjective evolutionary algorithm based on decision variable analyses (MOEA/DVA), extend graph-based differential grouping (gDG) to MOLSOPs, and test the method on many MOLSOPs. The experimental results show that mogDG-shift can achieve 100% grouping accuracy for LSMOP and DTLZ as well as almost all WFG instances, which are much better than DVA. We further combine mogDG-shift with two representative multiobjective evolutionary algorithms: the multiobjective evolutionary algorithm based on decomposition (MOEA/D) and the non-dominated sorting genetic algorithm II (NSGA-II). Compared with the original algorithms, the algorithms combined with mogDG-shift show improved optimization performance.

1. Introduction

In many real-world problems, it is necessary to consider various objectives simultaneously. Such problems can be treated as multiobjective optimization problems (MOPs). In an MOP, the various objectives always conflict with each other, and a set of possible solutions are required. Because of their ability to generate a set of solutions and their insensitivity to the shape of the Pareto front (PF), multiobjective evolutionary algorithms (MOEAs) [1,2] are capable of solving MOPs, and consequently, MOEAs have been applied to fields such as financial problems [3], satellite communications [4], industrial problems [5,6], data mining [7,8], etc.

With the advent of "big data", the dimensionality of MOPs is increasing. Many real-world problems can be treated as multiobjective large-scale optimization problems (MOLSOPs), such as the multiobjective large-scale recommendation problem [9]. An MOLSOP includes numerous variables, which challenges traditional MOEAs, such as the multiobjective evolutionary algorithm based on decomposition (MOEA/D) [10] and non-dominated sorting genetic algorithm II (NSGA-II) [11]. Several studies conducted on large-scale global optimization problems (LSGOPs) using approaches that allocate variables to multiple groups and optimize them under the cooperative coevolutionary (CC) [12,13] framework have shown good results. In this paper, to facilitate the more effective optimization of MOLSOPs, we focus on applying graph-based

* Corresponding author. Key Laboratory of Machine Intelligence and Advanced Computing (Sun Yat-sen University), Ministry of Education, Guangzhou 510006, China.
** Corresponding author. Beijing Advanced Innovation Center for Soft Matter Science and Engineering, Beijing University of Chemical Technology, Beijing 100029, China.
E-mail address: isslyb@mail.sysu.edu.cn (Y. Ling).

https://doi.org/10.1016/j.swevo.2019.100626
Received 17 December 2016; Received in revised form 18 August 2019; Accepted 12 November 2019
Available online 13 December 2019

differential grouping (gDG) [14] to these large-scale problems utilizing the CC framework which is conducive to resolving the big data problem.

Additionally, in MOPs, the variable properties [15,16] should be considered, which is not an issue in global optimization problems (GOPs). Position variables affect the diversity of the solutions, distance variables control the convergence of the solutions, while mixed variables affect both diversity and convergence. In the multiobjective evolutionary algorithm based on decision variable analyses (MOEA/DVA) [16], a grouping method for MOLSOPs called decision variable analyses (DVA) has been proposed. In DVA, the variables are first classified as position variables, distance variables or mixed variables. Then, the distance variables are separated based on their interactions. However, in DVA, the individuals are randomly initialized; thus, the results of the analysis may be unstable. In addition, the interaction learning is not precise, and the corresponding non-separable groups cannot be correctly formed.

In GOPs, all variables should be optimized to obtain the single optimal (near-optimal) value. In MOPs, there is no need to optimize variables affecting the diversity; however, there is a need to assign different values to comprehensively approximate the PF. To converge to the Pareto optimal front (POF), the variables affecting the convergence should be optimized. Therefore, we allocate all diversity-related variables to one group, while we separate the convergence-related variables into several groups according to the interactions among them.

Many methods for grouping variables have emerged, such as fixed grouping [12], random grouping [17], the Delta method [18], dynamic grouping [19], differential grouping (DG) [20], global differential grouping (GDG) [21], gDG [14], an improved variant of DG (DG2) [22], etc. In DG-type methods, the interaction between each pair of variables is analyzed prior to optimization, which yields good grouping precision. gDG normalizes the differences and groups variables in the same connected subcomponents of the constructed graph together. This approach can correctly group all non-separable variables in the CEC′10 test suite [23].

Considering the accuracy of gDG, we extend it to MOLSOPs. In contrast to LSGOPs, in MOLSOPs, there are several objectives. For each objective, we learn the interactions among all variables. Then, we combine the interactions in all objectives together: if two variables interact with each other with respect to at least one objective, we consider there to be an interaction between them.

The contributions of this paper can be summarized as follows:

1) We propose a new method called multiobjective graph-based differential grouping with shift (mogDG-shift) to decompose the variables in MOLSOPs.
2) DVA and gDG are modified and combined to better recognize the properties of variables and the interactions among them and correctly form non-separable groups.
3) We examine the grouping accuracy of mogDG-shift on MOLSOPs. It is verified that all non-separable variables can be recognized and that the corresponding groups can be correctly formed for LSMOP and DTLZ as well as almost all WFG instances. Compared with DVA, which is a state-of-the-art method, and the extended DG2, the precision of mogDG-shift is better, and less FEs are required.
4) We combine mogDG-shift with MOEA/D and NSGA-II, and better performance is achieved.

The remainder of this paper is organized as follows. Section 2 provides the preliminary knowledge for this paper. The test suite used to validate the mogDG-shift method is introduced in Section 3. Section 4 presents the mogDG-shift method in detail. We perform grouping experiments in Section 5. Section 6 describes the optimization experiments and analyses. Additional experimentation is provided in Section 7. Finally, Section 8 concludes this paper.

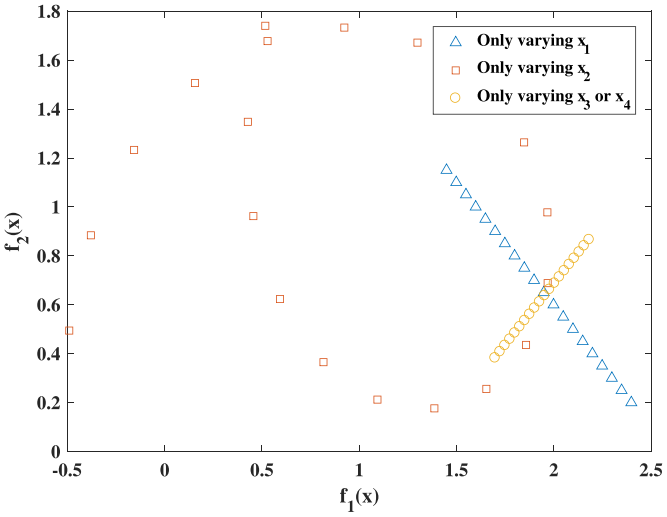

Fig. 1. Illustration of the sampling of points for the MOP formulated in Eq. (1) via changing one variable and fixing the others.

2. Preliminaries

2.1. Variable properties and separability

The variables in an MOP can be classified into three categories:

- position variables, which affect diversity;
- distance variables, which affect convergence; and
- mixed variables, which simultaneously affect diversity and convergence.

For example, consider the following problem:

$$\begin{cases} f_1(\mathbf{x}) = & x_1 - \cos(2.2\pi x_2) + x_2(x_3 + x_4) \\ f_2(\mathbf{x}) = & 1 - x_1 + \sin(2.2\pi x_2) + x_2(x_3 + x_4) \end{cases} \tag{1}$$

s.t. $x_i \in [0,1], i = 1,2,3,4$

By varying the variables, we can obtain Fig. 1. When only x_1 is varied, the generated solutions are non-dominated with respect to each other; consequently, x_1 is a position variable. By contrast, only domination relations are observed among the solutions generated by varying x_3 or x_4; therefore, these are distance variables. Finally, varying x_2 affects both convergence and diversity; therefore, it is a mixed variable.

When all variables are independent of each other, then the corresponding problem is fully separable. Fully separable problems are easy to solve because each variable can be optimized individually without considering the other variables. By contrast, in fully non-separable problems, each variable interacts with all other variables; therefore, to find the optimal value of each variable, the interactions with all other variables must be considered. These two cases represent the extreme conditions. Between these cases, for partially non-separable problems, the variables can be divided into several groups such that the variables within each group interact with each other but no interdependence exists among groups. For the MOP described in Eq. (1), x_1 is independent, but x_2, x_3 and x_4 interact with each other. Thus, it is a partially non-separable problem.

2.2. Cooperative coevolutionary (CC) framework

In the CC framework, let $\boldsymbol{X} = \{x_1, x_2, \ldots, x_{nDim}\}$ denote the set of all variables. Here, *nDim* is the number of variables, which can be very large (usually more than 100 [16]). Then, $\boldsymbol{X}$ is decomposed into several groups (species), denoted by $\boldsymbol{x}_{i,j}$, $i = 1,2,\ldots,NS$ and $j = 1,2,\ldots,NP$, where *NS* is the number of species and *NP* denotes the population size.

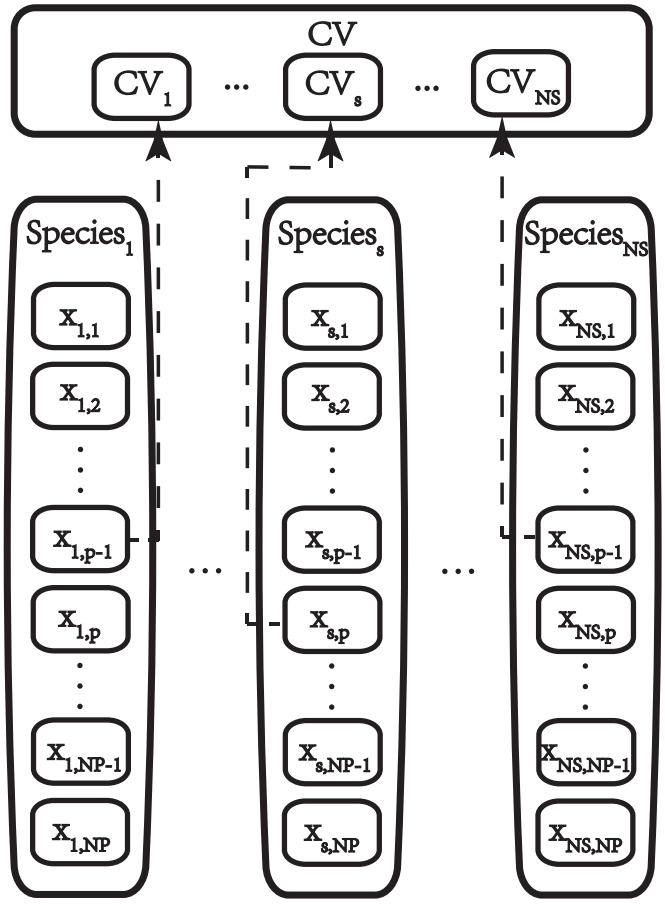

Fig. 2. CC framework.

Rather than optimizing all variables $\boldsymbol{X}$ as a single group, the CC framework optimizes the various species in a cooperative way. As illustrated in Fig. 2, each variable group is optimized as a species. To evaluate the offspring, the context vector (*CV*) containing all of the best solutions for all species is used. This approach is feasible for GOPs; however, because an MOP requires a set of solutions, several *CV*s are needed.

3. Large-scale multiobjective and many-objective test problems (LSMOPs)

Many multiobjective test suites have been developed, such as the Deb-Thiele-Laumanns-Zitzler (DTLZ) [24], Walking Fish Group (WFG) [15], and UF [25] suites. However, the test instances included in these test suites cannot be characterized as MOLSOPs. Recently, a collection of large-scale multiobjective and many-objective test problems (LSMOPs) [26] was proposed. These LSMOPs were constructed based on many concepts related to large-scale global optimization test suites (CEC′10 [23], CEC′13 [27], etc.); thus, they are quite suitable for testing the proposed mogDG-shift method.

The collection of LSMOPs includes 9 test problems. Each problem has the following form:

$$\begin{cases} f_1(\boldsymbol{x}) = h_1\left(\boldsymbol{x}^f\right)\left(1+g_1\left(\boldsymbol{x}^g\right)\right) \\ f_2(\boldsymbol{x}) = h_2\left(\boldsymbol{x}^f\right)\left(1+g_2\left(\boldsymbol{x}^g\right)\right) \\ \cdots \\ f_M(\boldsymbol{x}) = h_M\left(\boldsymbol{x}^f\right)\left(1+g_M\left(\boldsymbol{x}^g\right)\right) \end{cases} \tag{2}$$

where $f_i, i = 1, 2, \ldots, M$ are the objective functions; M is the number of objectives; h_i are the shape functions (influencing diversity), which control the shape of the Pareto-optimal front; and g_i are the landscape functions (influencing convergence), which define the fitness landscape. $\boldsymbol{x}$ is the solution vector, which consists of $\boldsymbol{x}^f$ and $\boldsymbol{x}^g$, where $\boldsymbol{x}^f \bigcap \boldsymbol{x}^g = \phi$, $\boldsymbol{x}^f \in [0,1]^{M-1}$ and $\boldsymbol{x}^g \in [0,10]^{D-M+1}$; here, $D \approx 100 \times M$ is the number of variables. The lower and upper boundaries, $\boldsymbol{X}^l$ and $\boldsymbol{X}^u$, have the following forms:

$$\boldsymbol{X}^l = (0, 0, \ldots, 0) \tag{3}$$

$$\boldsymbol{X}^u = \left(\underbrace{1, 1, \ldots, 1}_{M-1}, \underbrace{10, 10, \ldots, 10}_{D-M+1}\right) \tag{4}$$

The definition of each test problem is shown in Table 1, in which g^I and g^{II} represent two kinds of landscape functions used in each test instance, $\boldsymbol{C}$ denotes the correlation matrix, $\boldsymbol{H}$ denotes the shape function and L is the linkage function. In the following, the detailed description will be provided.

Table 1
Definitions of the LSMOPs.

Instance	g^I	g^{II}	$\boldsymbol{C}$	$\boldsymbol{H}$	L
LSMOP1	η_1	η_1	$\boldsymbol{C}_1$	$\boldsymbol{H}_1$	L_1
LSMOP2	η_5	η_2	$\boldsymbol{C}_1$	$\boldsymbol{H}_1$	L_1
LSMOP3	η_4	η_3	$\boldsymbol{C}_1$	$\boldsymbol{H}_1$	L_1
LSMOP4	η_6	η_5	$\boldsymbol{C}_1$	$\boldsymbol{H}_1$	L_1
LSMOP5	η_1	η_1	$\boldsymbol{C}_2$	$\boldsymbol{H}_2$	L_2
LSMOP6	η_3	η_2	$\boldsymbol{C}_2$	$\boldsymbol{H}_2$	L_2
LSMOP7	η_6	η_3	$\boldsymbol{C}_2$	$\boldsymbol{H}_2$	L_2
LSMOP8	η_5	η_1	$\boldsymbol{C}_2$	$\boldsymbol{H}_2$	L_2
LSMOP9	η_1	η_6	$\boldsymbol{C}_3$	$\boldsymbol{H}_3$	L_2

Table 2
Characteristics of the subproblems.

#	Subproblem	Modality	Separability
η_1	Sphere function	Unimodal	Separable
η_2	Schwefel function	Unimodal	Non-separable
η_3	Rosenbrock function	Multi-modal	Non-separable
η_4	Rastrigin function	Multi-modal	Separable
η_5	Griewank function	Multi-modal	Non-separable
η_6	Ackley's function	Multi-modal	Separable

3.1. The landscape functions

In LSMOPs, 6 functions are utilized:

$$\begin{cases} \eta_1 &= \sum_{i=1}^{|\boldsymbol{x}|} x_i^2 \\ \eta_2 &= \max_{i=1}^{|\boldsymbol{x}|} \operatorname{abs}(x_i) \\ \eta_3 &= \sum_{i=1}^{|\boldsymbol{x}|-1} \left[100\left(x_{i+1} - x_i^2\right)^2 + (x_i - 1.0)^2\right] \\ \eta_4 &= \sum_{i=1}^{|\boldsymbol{x}|} \left[x_i^2 - 10.0 \times \cos(2\pi x_i) + 10.0\right] \\ \eta_5 &= \sum_{i=1}^{|\boldsymbol{x}|} \left(x_i^2\right)/4000 - \prod_{i=1}^{|\boldsymbol{x}|} \cos\left(x_i/\sqrt{i}\right) + 1 \\ \eta_6 &= 20 - 20 \times e^{-0.2\sqrt{\frac{1}{|\boldsymbol{x}|}\sum_{i=1}^{|\boldsymbol{x}|} x_i^2}} - \\ & \quad e^{\frac{1}{|\boldsymbol{x}|}\sum_{i=1}^{|\boldsymbol{x}|} \cos(2\pi x_i)} + e \end{cases} \tag{5}$$

where $\boldsymbol{x}$ is the input variable vector.

The characteristics of these subproblems are summarized in Table 2.

Specifically, there are M subcomponents, denoted as $\overline{g}_i\left(\boldsymbol{x}_i^g\right)$, $i = 1, 2, \ldots, M$; accordingly, variables in $\boldsymbol{x}^g$ are divided into M parts:

$$\boldsymbol{x}^g = \left(\boldsymbol{x}_1^g, \boldsymbol{x}_2^g, \ldots, \boldsymbol{x}_M^g\right) \tag{6}$$

and $x_i^g \bigcap x_j^g = \phi$ for $i,j \in [1,M], i \neq j$. The calculation of $\overline{g}_i\left(x_i^g\right)$ is detailed as follows:

$$\overline{g}_i\left(x_i^g\right) = \frac{1}{n_k}\sum_{j=1}^{n_k}\frac{\overline{g}_i^{\bullet}\left(x_{i,j}^g\right)}{\left|x_{i,j}^g\right|} \tag{7}$$

$$x_i^g = \left(x_{i,1}^g, x_{i,2}^g, \ldots, x_{i,n_k}^g\right) \tag{8}$$

where $\overline{g}_i^{\bullet}$ has the following form:

$$\overline{g}_i^{\bullet} = \begin{cases} g^I & i \text{ is odd} \\ g^{II} & i \text{ is even} \end{cases} \tag{9}$$

Additionally, each objective may not relate to all of these M subcomponents; instead, the relationships between objectives and subcomponents are controlled by the correlation matrix $\boldsymbol{C}$, which has the following form:

$$\boldsymbol{C} = \begin{pmatrix} c_{1,1} & c_{1,2} & \cdots & c_{1,M} \\ c_{2,1} & c_{2,2} & \cdots & c_{2,M} \\ \vdots & \vdots & \ddots & \vdots \\ c_{M,1} & c_{M,2} & \cdots & c_{M,M} \end{pmatrix} \tag{10}$$

where with respect to $i,j \in [1,M]$, $c_{i,j} = 0$ denotes that objective function $f_i(\boldsymbol{x})$ and variable group x_j^g are not interrelated, whereas for other values of $c_{i,j}$, they are related. $g_i(\boldsymbol{x}^g)$, $i = 1,2,\ldots,M$ can be calculated as follows:

$$g_i\left(\boldsymbol{x}^g\right) = \sum_{j=1}^{M} c_{i,j}\overline{g}_j\left(x_j^g\right) \tag{11}$$

Specifically, there are three particular matrices utilized in the test instances of LSMOPs:

1) Separable Correlations:

$$\boldsymbol{C}_1 = \begin{pmatrix} 1 & 0 & \cdots & 0 \\ 0 & 1 & \cdots & 0 \\ \vdots & \vdots & \ddots & \vdots \\ 0 & 0 & \cdots & 1 \end{pmatrix} \tag{12}$$

In this case, all M objective functions and M variable groups form a one-to-one match, and objective i is only related to variable group i; by contrast, different objective functions have no correlated variable group(s).

2) Overlapped Correlations:

$$\boldsymbol{C}_2 = \begin{pmatrix} 1 & 1 & 0 & \cdots & 0 \\ 0 & 1 & 1 & 0 & \vdots \\ \vdots & 0 & \ddots & \ddots & 0 \\ \vdots & 0 & 0 & 1 & 1 \\ 0 & \cdots & \cdots & 0 & 1 \end{pmatrix} \tag{13}$$

In this case, objective function i is related to two variable groups: i and $i+1$, except the last one, which is only relating to variable group M. Therefore, the adjacent objective functions have a correlated variable group.

3) Full Correlations:

$$\boldsymbol{C}_3 = \begin{pmatrix} 1 & 1 & \cdots & 1 \\ 1 & 1 & \cdots & 1 \\ \vdots & \vdots & \ddots & \vdots \\ 1 & 1 & \cdots & 1 \end{pmatrix} \tag{14}$$

In this case, each objective function is correlated to all M variable groups.

3.2. The shape functions

Three formulations are utilized:

1) Linear PF (Fig. 3a and b):

$$\boldsymbol{H}_1\left(\boldsymbol{x}^f\right): \begin{cases} h_1\left(\boldsymbol{x}^f\right) = x_1^f \ldots x_{M-1}^f \\ h_2\left(\boldsymbol{x}^f\right) = x_1^f \ldots \left(1 - x_{M-1}^f\right) \\ \cdots \\ h_{M-1}\left(\boldsymbol{x}^f\right) = x_1^f\left(1 - x_2^f\right) \\ h_M\left(\boldsymbol{x}^f\right) = \left(1 - x_1^f\right) \end{cases} \tag{15}$$

2) Convex PF (Fig. 3c and d):

$$\boldsymbol{H}_2\left(\boldsymbol{x}^f\right): \begin{cases} h_1\left(\boldsymbol{x}^f\right) = \cos\left(\frac{\pi}{2}x_1^f\right)\ldots\cos\left(\frac{\pi}{2}x_{M-2}^f\right)\cos\left(\frac{\pi}{2}x_{M-1}^f\right) \\ h_2\left(\boldsymbol{x}^f\right) = \cos\left(\frac{\pi}{2}x_1^f\right)\ldots\cos\left(\frac{\pi}{2}x_{M-2}^f\right)\sin\left(\frac{\pi}{2}x_{M-1}^f\right) \\ h_3\left(\boldsymbol{x}^f\right) = \cos\left(\frac{\pi}{2}x_1^f\right)\ldots\sin\left(\frac{\pi}{2}x_{M-2}^f\right) \\ \cdots \\ h_{M-1}\left(\boldsymbol{x}^f\right) = \cos\left(\frac{\pi}{2}x_1^f\right)\sin\left(\frac{\pi}{2}x_2^f\right) \\ h_M\left(\boldsymbol{x}^f\right) = \sin\left(\frac{\pi}{2}x_1^f\right) \end{cases}$$

3) Disconnected PF (Fig. 3e and f):

$$\boldsymbol{H}_3\left(\boldsymbol{x}^f\right): \begin{cases} h_1\left(\boldsymbol{x}^f\right) = x_1^f \\ h_2\left(\boldsymbol{x}^f\right) = x_2^f \\ \cdots \\ h_{M-1}\left(\boldsymbol{x}^f\right) = x_{M-1}^f \\ h_M\left(\boldsymbol{x}^f\right) = \left(M - \sum_{i=1}^{M-1}\frac{x_i^f\left(1+\sin\left(3\pi x_i^f\right)\right)}{2+g_M\left(\boldsymbol{x}^g\right)}\right) \\ \qquad \times\left[2+g_M\left(\boldsymbol{x}^g\right)\right] \end{cases} \tag{16}$$

3.3. The variable linkage

Each variable in $\boldsymbol{x}^g$ is correlated with the first variable. In the test instances of LSMOPs, there are two kinds of linkages:

1) Linear linkage function:

$$L_1\left(\boldsymbol{x}^g\right) = \left(1 + \frac{i}{\left|\boldsymbol{x}^f\right| + \left|\boldsymbol{x}^g\right|}\right) \times \left(x_i^g - X_i^l\right) - x_1^f \times \left(X_i^u - X_i^l\right) \tag{17}$$

2) Nonlinear linkage function:

$$L_2\left(\boldsymbol{x}^g\right) = \left(1 + \cos\left(\frac{0.5i\pi}{\left|\boldsymbol{x}^f\right| + \left|\boldsymbol{x}^g\right|}\right)\right) \times \left(x_i^g - X_i^l\right) - x_1^f \times \left(X_i^u - X_i^l\right) \tag{18}$$

4. Multiobjective graph-based differential grouping with shift (mogDG-shift)

In this section, we introduce the proposed multiobjective graph-based differential grouping with shift (mogDG-shift) technique. In

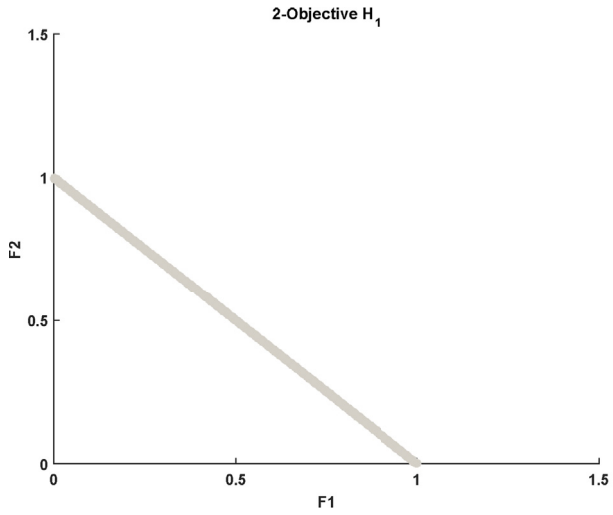

(a)

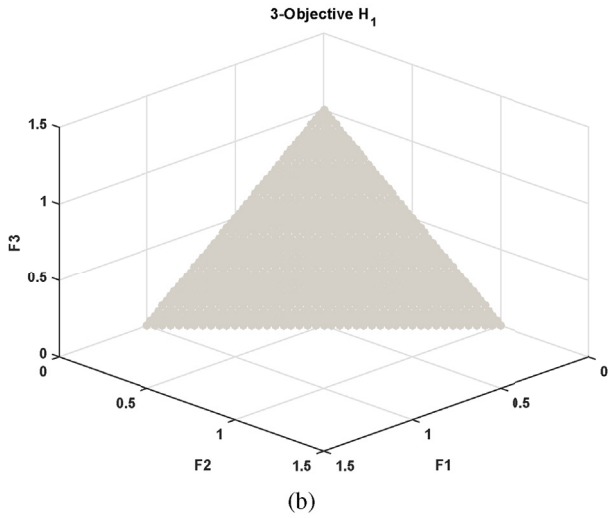

(b)

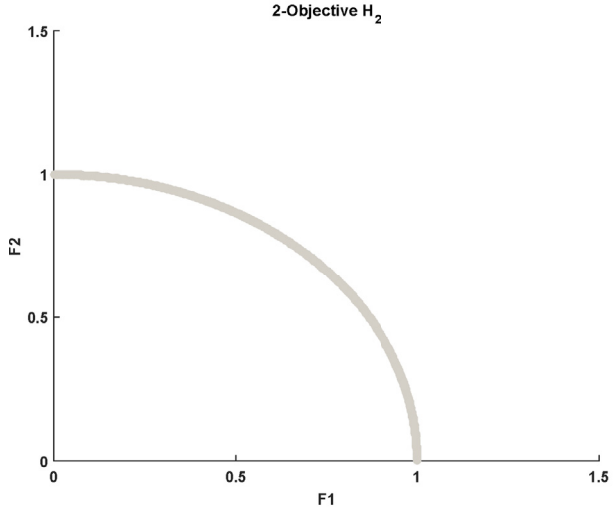

(c)

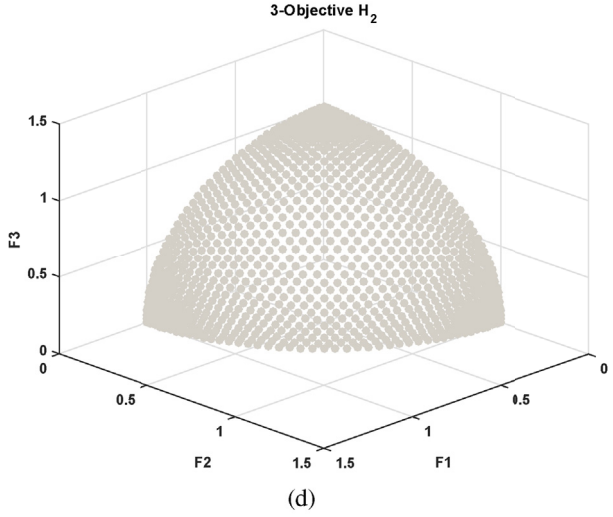

(d)

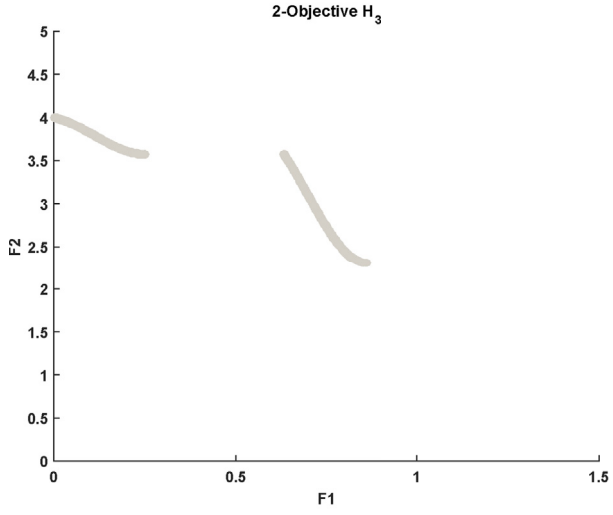

(e)

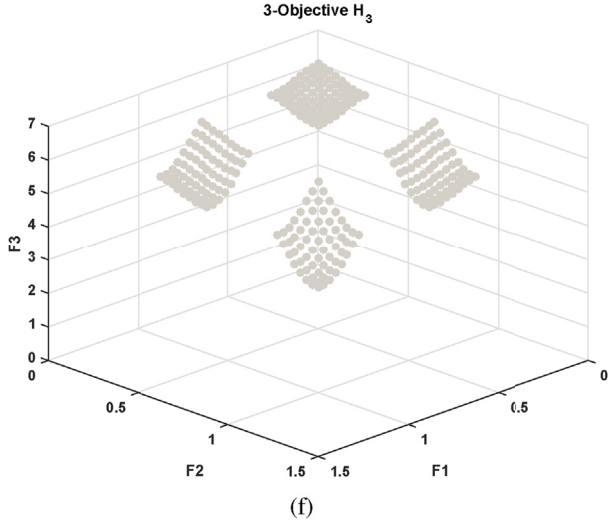

(f)

Fig. 3. Visualizations of the 2-/3-objective shape functions.

mogDG-shift, there are three components: property analysis, interaction learning and graph-based grouping.

Algorithm 1 Property Analysis.

Input: number of variables: $nDim$; number of objectives: $nObj$; number of samples: N_{PA}; upper boundary: $\boldsymbol{X}^u$; lower boundary: $\boldsymbol{X}^l$.
Output: diversity-related variables: $\boldsymbol{S}_D$; convergence-related variables: $\boldsymbol{S}_C$.

$\boldsymbol{S}_D = \boldsymbol{S}_C = \phi$;
for $i = 1$ *to* $nDim$ **do**
  Solution set $\boldsymbol{S} = \phi$;
  for $j = 1$ *to* N_{PA} **do**
    for $k = 1$ *to* $nDim$ **do**
      if $k == i$ **then**
        $\boldsymbol{Y}_k = \frac{(j - 1 + \frac{1}{\gamma^P})}{N_{PA}} \times \left(\boldsymbol{X}_k^u - \boldsymbol{X}_k^l\right) + \boldsymbol{X}_k^l$;
      else
        $\boldsymbol{Y}_k = 0.5 \times \left(\boldsymbol{X}_k^l + \boldsymbol{X}_k^u\right) + \boldsymbol{\varepsilon}_k^P$;
    $\boldsymbol{S} = \boldsymbol{S} \bigcup \boldsymbol{Y}$;
  $flag = false$;
  for $j = 1$ *to* N_{PA} **do**
    for $k = j + 1$ *to* N_{PA} **do**
      if $\boldsymbol{S}_j$ *and* $\boldsymbol{S}_k$ *are non-dominated to each other* **then**
        $flag = true$;
  if $flag$ **then**
    $\boldsymbol{S}_D = \boldsymbol{S}_D \bigcup \{i\}$;
  else
    $\boldsymbol{S}_C = \boldsymbol{S}_C \bigcup \{i\}$;

4.1. Property analysis

By analyzing the effect of each variable on the solutions, we can classify each variable as diversity-related or convergence-related. Position variables and mixed variables are considered diversity-related, whereas the remaining variables are characterized as convergence-related. The implementation is shown in Algorithm 1. For the ith variable, we uniformly sample N_{PA} values within its search range $\left[\boldsymbol{X}_i^l, \boldsymbol{X}_i^u\right]$ and set the other variables to middle values $\boldsymbol{X}_i^m$ of their search ranges plus shifts $\boldsymbol{\varepsilon}_i^P$, where $\boldsymbol{X}_i^l$ ($\boldsymbol{X}_i^u$) is the lower (upper) boundary of the ith variable, $\boldsymbol{X}_i^m = 0.5 \times \left(\boldsymbol{X}_i^l + \boldsymbol{X}_i^u\right)$, $i = 1, 2, \ldots, nDim$, and ε_i^P denotes a shift value for property analysis, formulated as follows:

$$\varepsilon_i^P = \left(X_i^u - X_i^l\right) / \gamma^P \tag{19}$$

where γ^P denotes a parameter.

Thus, we obtain N_{PA} solutions that can be used to examine the property of the ith variable. If any two solutions among them are mutually non-dominated, then the ith variable is a diversity-related variable; otherwise, it is a convergence-related variable. For the MOP formulated in Eq. (1), through sampling, we can obtain a solutions set with respect to each variable, which corresponds to those points in Fig. 1. Thus, we can know that x_1 and x_2 are diversity-related variables, whereas x_3 and x_4 are convergence-related variables.

4.2. Interaction learning

The method gDG was proposed in Ref. [14] and achieves perfect grouping accuracy for LSGOPs in the CEC′10 suite [23]. Therefore, we extend this technique to interaction learning for MOLSOPs.

The entire process is detailed in Algorithm 2, in which $Ind(i)$ returns the true index of the i-th convergence variable. To detect the interactions, we first construct a solution $\boldsymbol{X}_0$ as follows:

Algorithm 2 Interaction Learning.

Input: number of convergence-related variables: $nCov$; number of objectives: $nObj$; upper boundary: $\boldsymbol{X}^u$; lower boundary: $\boldsymbol{X}^l$.
Output: correlation matrix: $\boldsymbol{M}_C$

. Initialize the maximal weights $\boldsymbol{W}_{max}$, and the minimal weights $\boldsymbol{W}_{min}$;
$\boldsymbol{X}_0 = \boldsymbol{X}^l + \boldsymbol{\Theta}^I$; $\boldsymbol{f}_0 = f(\boldsymbol{X}_0)$;
for $i = 1$ *to* $nCov$ **do**
  $\boldsymbol{X}_1 = \boldsymbol{X}_0$; $\boldsymbol{X}_{1,Ind(i)} = \boldsymbol{X}_{Ind(i)}^u - \boldsymbol{\varepsilon}_{Ind(i)}^I$; $\hat{\boldsymbol{f}}_i = f(\boldsymbol{X}_1)$;
  for $j = i + 1$ *to* $nCov$ **do**
    $\boldsymbol{X}_2 = \boldsymbol{X}_1$;
    $\boldsymbol{X}_{2,Ind(j)} = \boldsymbol{X}_{Ind(j)}^u - \boldsymbol{\varepsilon}_{Ind(j)}^I$;
    $\boldsymbol{F}_{i,j} = f(\boldsymbol{X}_2)$;
for $i = 1$ *to* $nCov$ **do**
  for $j = i + 1$ *to* $nCov$ **do**
    $\boldsymbol{\Delta}_1 = \boldsymbol{f}_0 - \hat{\boldsymbol{f}}_i$; $\boldsymbol{\Delta}_2 = \hat{\boldsymbol{f}}_j - \boldsymbol{F}_{i,j}$;
    for $l = 1$ *to* $nObj$ **do**
      $\boldsymbol{T}_{D,l,i,j} = \boldsymbol{T}_{D,l,j,i} = |\boldsymbol{\Delta}_{1,l} - \boldsymbol{\Delta}_{2,l}|$;
      if $\boldsymbol{W}_{min,l} > \boldsymbol{T}_{D,l,i,j}$ **then**
        $\boldsymbol{W}_{min,l} = \boldsymbol{T}_{D,l,i,j}$;
      if $\boldsymbol{W}_{max,l} < \boldsymbol{T}_{D,l,i,j}$ **then**
        $\boldsymbol{W}_{max,l} = \boldsymbol{T}_{D,l,i,j}$;
for $i = 1$ *to* $nCov$ **do**
  for $j = i + 1$ *to* $nCov$ **do**
    $\boldsymbol{M}_{C,i,j} = \boldsymbol{M}_{C,j,i} = 0$;
    for $l = 1$ *to* $nObj$ **do**
      if $(\boldsymbol{W}_{max,l} - \boldsymbol{W}_{min,l}) > \omega$ **then**
        $\boldsymbol{T}_{D,l,i,j} = \boldsymbol{T}_{D,l,j,i} = \boldsymbol{W}_{min,l} + \frac{\boldsymbol{T}_{D,l,i,j} - \boldsymbol{W}_{min,l}}{\boldsymbol{W}_{max,l} - \boldsymbol{W}_{min,l}}$;
      if $\boldsymbol{T}_{D,l,i,j} > \omega$ **then**
        $\boldsymbol{M}_{C,i,j} = \boldsymbol{M}_{C,j,i} = 1$;

$$\boldsymbol{X}_0 = \boldsymbol{X}^l + \boldsymbol{\Theta}^I \tag{20}$$

where $\boldsymbol{\Theta}^I$ is the shift vector and

$$\boldsymbol{\Theta}^I = \left(\varepsilon_1^I, \ldots, \varepsilon_i^I, \ldots, \varepsilon_{nDim}^I\right) \tag{21}$$

$$\varepsilon_i^I = \left(X_i^u - X_i^l\right) / \gamma^I \tag{22}$$

where γ^I is a predefined parameter and ε_i^I is the shift value of the ith variable. We store $f(\boldsymbol{X}_0)$ in $\boldsymbol{f}_0$. Based on $\boldsymbol{X}_0$, we set each convergence-related variable i to $\boldsymbol{X}_{Ind(i)}^u - \boldsymbol{\varepsilon}_{Ind(i)}^I$, and these $nCov$ function results are stored in $\hat{\boldsymbol{f}}$. Then, $\boldsymbol{F}$ is calculated by setting two different convergence-related variables to the upper boundary minus the shift values, that is, $\boldsymbol{F}_{i,j} = f(\boldsymbol{X}_2)$. Here, $\boldsymbol{X}_2$ is the same as $\boldsymbol{X}_0$, except that the ith and jth convergence-related variables are set to $\boldsymbol{X}_{Ind(i)}^u - \boldsymbol{\varepsilon}_{Ind(i)}^I$ and $\boldsymbol{X}_{Ind(j)}^u - \boldsymbol{\varepsilon}_{Ind(j)}^I$, respectively. For each two convergence-related variables, based on the stored $\boldsymbol{f}_0$, $\hat{\boldsymbol{f}}$ and $\boldsymbol{F}$, $\boldsymbol{\Delta}_1$ and $\boldsymbol{\Delta}_2$ are computed. Then, the differences between $\boldsymbol{\Delta}_1$ and $\boldsymbol{\Delta}_2$ are computed for each objective. Normalization is also performed for each objective. Finally, when the normalized difference is beyond the threshold ω with respect to at least one

objective function, we assume that the ith and jth convergence-related variables are interacting.

Inspired by DG2 [22], in Algorithm 2, the function values can be reused. By applying this idea, compared to gDG, the number of fitness evaluations (FEs) consumed is halved.

In gDG [14], the solution vector is initialized to the boundary values, which is not an issue in the analysis of LSGOPs. However, MOPs include diversity-related variables. Moreover, in an LSMOP, their values are not shifted. Thus, when boundary values are assigned, the objective values will be 0, and none of the interdependences between other pairs of variables can be detected. For example, LSMOP2 with 2 objectives can be expressed as follows:

$$\begin{cases} f_1(\boldsymbol{x}) = h_1\left(\boldsymbol{x}^f\right)\left(1+g_1\left(\boldsymbol{x}^g\right)\right) \\ f_2(\boldsymbol{x}) = h_2\left(\boldsymbol{x}^f\right)\left(1+g_2\left(\boldsymbol{x}^g\right)\right) \end{cases} \tag{23}$$

$$\begin{cases} h_1\left(\boldsymbol{x}^f\right) = x_1 \\ h_2\left(\boldsymbol{x}^f\right) = 1 - x_1 \end{cases} \tag{24}$$

s.t. $x_1 \in [0,1],\ x_i \in [0,10],\ i = 2,\ldots,nDim$

where $\boldsymbol{x}^f$ is the set of variables that control the shape of the solution set, known as the diversity-related variables, and $\boldsymbol{x}^g$ is the set of variables that control the convergence of the solution set, known as the convergence-related variables. As shown in Eq. (24), there is only one diversity-related variable, x_1. When the boundary value 0 (or 1) is assigned to x_1, then $h_1\left(\boldsymbol{x}^f\right)$ (or $h_2\left(\boldsymbol{x}^f\right)$) will be 0, and accordingly, $f_1(\boldsymbol{x})$ (or $f_2(\boldsymbol{x})$) will be 0. In order to test the interdependence between two convergence-related variables i and j in $\boldsymbol{x}^g$, the value of x_1 is fixed to the lower boundary 0. Then, gDG produces four solution vectors:

$$\begin{cases} \hat{\boldsymbol{X}}_1 = \left(0, \boldsymbol{X}_2^l, \ldots, \boldsymbol{X}_i^l, \ldots, \boldsymbol{X}_j^l, \ldots, \boldsymbol{X}_{nDim}^l\right) \\ \hat{\boldsymbol{X}}_2 = \left(0, \boldsymbol{X}_2^l, \ldots, \boldsymbol{X}_i^u, \ldots, \boldsymbol{X}_j^l, \ldots, \boldsymbol{X}_{nDim}^l\right) \\ \hat{\boldsymbol{X}}_3 = \left(0, \boldsymbol{X}_2^l, \ldots, \boldsymbol{X}_i^l, \ldots, \boldsymbol{X}_j^m, \ldots, \boldsymbol{X}_{nDim}^l\right) \\ \hat{\boldsymbol{X}}_4 = \left(0, \boldsymbol{X}_2^l, \ldots, \boldsymbol{X}_i^u, \ldots, \boldsymbol{X}_j^m, \ldots, \boldsymbol{X}_{nDim}^l\right) \end{cases} \tag{25}$$

Next, their differences are calculated as follows:

$$\begin{cases} \boldsymbol{\Delta}_{1,1} = f_1\left(\hat{\boldsymbol{X}}_1\right) - f_1\left(\hat{\boldsymbol{X}}_2\right) \\ \boldsymbol{\Delta}_{2,1} = f_1\left(\hat{\boldsymbol{X}}_3\right) - f_1\left(\hat{\boldsymbol{X}}_4\right) \end{cases} \tag{26}$$

Finally, $\boldsymbol{\omega}_{1,i,j}$ is computed:

$$\boldsymbol{\omega}_{1,i,j} = |\boldsymbol{\Delta}_{1,1} - \boldsymbol{\Delta}_{2,1}| \tag{27}$$

After normalization, if $\boldsymbol{\omega}_{1,i,j}$ is greater than a predefined threshold value, $\boldsymbol{\omega}$, we determine that x_i and x_j interact with each other for the 1st objective. However, because x_1 is fixed to its lower boundary, which is 0, $f_1\left(\hat{\boldsymbol{X}}_1\right) = f_1\left(\hat{\boldsymbol{X}}_2\right) = f_1\left(\hat{\boldsymbol{X}}_3\right) = f_1\left(\hat{\boldsymbol{X}}_4\right) = 0$. Therefore, $\boldsymbol{\omega}_{1,i,j} = 0$ for any two variables in $\boldsymbol{x}^g$; consequently, with respect to the 1st objective, for convergence-related variables, any interdependence between them will not be detected. Additionally, in $\hat{\boldsymbol{X}}_3$ and $\hat{\boldsymbol{X}}_4$, gDG sets the jth variable to the middle value $\boldsymbol{X}_j^m$, while in mogDG-shift, it is set to $\boldsymbol{X}_j^u - \varepsilon_j^I$, facilitating the reuse of function values and the reduction of FEs similar to DG2 [22].

4.3. Graph-based grouping [14]

During the property analysis stage, the variables are classified as either diversity-related or convergence-related. Then, in the interaction learning stage, we obtain the correlation matrix. In the final stage, we construct a graph based on the correlation matrix and assign variables in the same connected subcomponents to the same groups.

The connected subcomponents to which each variable belongs can be inspected by applying a depth-first search or breadth-first search based on the correlation matrix $\boldsymbol{M}_C$ obtained from Algorithm 2. Finally, each variable is assigned to a connected subcomponent, and variables in the same subcomponent will be assigned to the same group.

Table 3
Variable Analysis Results of N_{PA} in mogDG-shift/DVA of 30 Runs.

	2-obj			3-obj		
	2	10	20	2	10	20
LSMOP1	1/1	1/1	1/1	2/2	2/2	2/2
LSMOP2	1/1	1/1	1/1	2/2	2/2	2/2
LSMOP3	1/1	1/1	1/1	2/1.97	2/2	2/2
LSMOP4	1/1	1/1	1/1	2/2	2/2	2/2
LSMOP5	1/0.87	1/1	1/1	2/2	2/2	2/2
LSMOP6	1/1	1/1	1/1	1/1.63	2/2	2/2
LSMOP7	1/0.20	1/1	1/1	2/2	2/2	2/2
LSMOP8	1/0.87	1/1	1/1	2/2	2/2	2/2
LSMOP9	1/1	1/1	1/1	1/1.87	2/2	2/2

Table 4
Grouping groundtruth of 2-/3-objective LSMOPs.

Function	Sep Vars	Non-sep Vars	Non-sep Groups
LSMOP1	205/305	0/0	0/0
LSMOP2	0/0	205/305	10/15
LSMOP3	60/150	145/155	5/5
LSMOP4	60/150	145/155	5/5
LSMOP5	205/305	0/0	0/0
LSMOP6	0/0	205/305	10/15
LSMOP7	60/150	145/155	5/5
LSMOP8	145/155	60/150	5/10
LSMOP9	205/305	0/0	0/0

5. Grouping experimentation

5.1. Parameters in mogDG-shift

There are four parameters in mogDG-shift: the sampling number N_{PA}, parameter γ^P, threshold ω and shift parameter γ^I.

The aim of variable property analysis is to classify variables as diversity-related (position variables and mixed variables) or convergence-related (distance variables) as introduced in Subsection 2.1 and detailed in Algorithm 1. For LSMOPs, the groundtruth is that the number of diversity-related variables is $nObj - 1$, all others are convergence-related variables, and there are no mixed variables. We simply set γ^P to 111.1. To test the influence of N_{PA} on the accuracy of property analysis, we use three different values: 2, 10 and 20; the lower the value, the smaller the number of FEs utilized. The results are listed in Table 3. For DVA, as the individuals are initialized randomly, the analysis may be unstable, while in mogDG-shift, the remaining variables which are not permuted are set to the middle values plus shift values as in Line 9 of Algorithm 1. According to DVA [16], we can simply set $N_{PA} = 20$.

Table 4 lists the groundtruth of variable groups with respect to the 2-/3-objective LSMOPs, in which LSMOP1, LSMOP5 and LSMOP9 are fully separable problems. Consequently, in the following experiments, the grouping accuracies of these problems are not analyzed. Tables 5 and 6 list the grouping results obtained by applying gDG directly to convergence-related variables of multiobjective problems, denoted as mogDG. It should be noted that, to avoid the situation in which $\boldsymbol{W}_{max} = \boldsymbol{W}_{min}$, the weights are normalized only when $\boldsymbol{W}_{max} - \boldsymbol{W}_{min} > 10^{-100}$. In these tables, the first four columns denote the name of the

Table 5
Variable Analysis Results Obtained Using mogDG on 2-objective LSMOPs with $\omega = 10^{-4}/10^{-6}/10^{-8}$.

Function	# Captured Non-sep Vars	# Formed Non-sep Groups	# Misplaced Vars	Grouping Accuracy
LSMOP1	145/145/145	1/1/1	0/0/0	−/−/−
LSMOP2	145/145/145	5/5/5	60/60/60	70.73%/70.73%/70.73%
LSMOP3	145/145/145	5/5/5	0/0/0	100.00%/100.00%/100.00%
LSMOP4	145/145/145	5/5/5	0/0/0	100.00%/100.00%/100.00%
LSMOP5	205/205/205	1/1/1	0/0/0	−/−/−
LSMOP6	60/205/205	5/10/10	145/0/0	29.27%/100.00%/100.00%
LSMOP7	145/205/205	5/10/10	0/0/0	100.00%/100.00%/100.00%
LSMOP8	60/60/60	5/5/5	0/0/0	100.00%/100.00%/100.00%
LSMOP9	145/145/145	5/5/5	0/0/0	−/−/−

Table 6
Variable Analysis Results Obtained Using mogDG on 3-objective LSMOPs with $\omega = 10^{-4}/10^{-6}/10^{-8}$.

Function	# Captured Non-sep Vars	# Formed Non-sep Groups	# Misplaced Vars	Grouping Accuracy
LSMOP1	85/85/85	1/1/1	0/0/0	−/−/−
LSMOP2	85/85/85	5/5/5	220/220/220	27.87%/27.87%/27.87%
LSMOP3	85/85/85	1/1/1	155/155/155	0.00%/0.00%/0.00%
LSMOP4	85/85/85	5/5/5	155/155/155	0.00%/0.00%/0.00%
LSMOP5	220/220/220	1/1/1	0/0/0	−/−/−
LSMOP6	65/220/220	5/10/10	240/85/85	21.31%/72.13%/72.13%
LSMOP7	155/220/220	5/10/10	0/0/0	100.00%/100.00%/100.00%
LSMOP8	65/65/65	5/5/5	85/85/85	43.33%/43.33%/43.33%
LSMOP9	155/155/155	5/5/5	0/0/0	−/−/−

test instance, the number of captured non-separable variables, the number of formed non-separable groups, and the number of misplaced variables (those true non-separable variables that are incorrectly recognized as separable ones), respectively. The last column is the grouping accuracy: if all non-separable variables are correctly recognized, we set it as 100.00% and the number of formed non-separable groups should be simultaneously taken into consideration to verify the grouping accuracy; otherwise, this value is the percentage of the recognized true non-separable variables with respect to the total number of true non-separable variables. If true separable variables are recognized as non-separable variables and non-separable groups are formed, we consider this to not affect the grouping accuracy.

In Table 5, for 2-objective instances, there are 5 non-separable groups in LSMOP2 that are not detected; for 3-objective instances in Table 6, 10, 5 and 5 non-separable groups are not detected in LSMOP2, LSMOP6 and LSMOP8, respectively, and none of the non-separable groups is detected in LSMOP3 or LSMOP4. To remedy this, the assigned values must be shifted from the boundary by $\mathbf{\Theta}^I$ (Eq. (21)).

For mogDG-shift, different γ^I values are tested: 11.1, 111.1 and 1111.1 (the grouping results with values of 11.1 and 1111.1 are detailed in the supplementary material). For each γ^I value, we analyze the sensitivity of mogDG-shift to ω. The results with the γ^I value of 111.1 (Tables 7 and 8) show that for a γ^I, we can find an ω to achieve a correct grouping. In the following experiments, we set $\gamma^I = 111.1$ and $\omega = 10^{-6}$ for the 2-/3-objective test instances. However, at the same time, some separable variables are classified as non-separable variables, and non-separable groups are formed. These results appear in LSMOP4, LSMOP7 and LSMOP9 (with 2/3 objectives). The variables are in subproblem η_6. From the expression of η_6 (Eq. (5)), we know that variables interact with one another because there are two power exponent functions.

DG2 [22] is a newly proposed powerful grouping methodology. To verify the superiority of our proposed mogDG-shift, we replace gDG in mogDG and mogDG-shift with DG2 to construct multiobjective DG2 (moDG2) and moDG2-shift, respectively, the grouping results of which are listed in Tables 9 and 10. For the 2-/3-objective test instances, moDG2 without the shift technique cannot guarantee the grouping accuracy of 100.00% for 2-objective LSMOP2 as well as 3-objective LSMOP2, LSMOP3, LSMOP4, LSMOP6 and LSMOP8. With a proper γ^I value, moDG2-shift can correctly recognize all non-separable variables; however, the number of formed non-separable groups is not correct (except for 2-objective LSMOP2), because several groups are formed from true separable variables and several true non-separable groups are merged into one group. In the following experiments, we simply set γ^I as 111.1 for moDG2-shift.

With the above parameter settings, we compare the grouping results of mogDG-shift and moDG2-shift to DVA in Table 11. Compared to mogDG-shift and moDG2-shift, many non-separable variables are not recognized, and the corresponding non-separable groups are not correctly formed. In addition, there are many more FEs consumed (Table 12).

5.2. Grouping size of separable variables

In the LSMOP test instances, there are many separable variables. These can be optimized one by one and arbitrarily formed into groups. When they are optimized individually, the FEs will be consumed rapidly. When they are optimized as a single group, the optimization result may be unsatisfying. To find a balance between FE consumption and the optimization performance, we perform experiments to find the best group size for separable variables.

We test six group sizes: 1 (optimized individually), 10, 30, 50 and ∞ (optimized in a single group). The result of the non-parametric tests [28,29] is listed in Table 13, where M and N denote CCMOEA/D-DE and CCNSGA–II–DE, respectively, and the detailed optimization results can be found in the supplementary material. Generally, the results show that setting the group size to 30 is the best choice for optimizing separable variables for LSMOP.

6. Optimization experimentation on LSMOPs

In this section, we optimize the 2-/3-objective test instances in LSMOP using NSGA–II–DE and MOEA/D-DE [30] and then compare those using the same algorithms but combined with mogDG-shift and moDG2-shift, denoted as CCNSGA–II–DE and CCMOEA/D-DE, as well as CC2NSGA–II–DE and CC2MOEA/D-DE, respectively.

Table 7
Variables Analysis Results Obtained Using mogDG-shift on 2-objective LSMOPs with $\omega = 10^{-4}/10^{-6}/10^{-8}, \gamma^I = 111.1$

Function	# Captured Non-sep Vars	# Formed Non-sep Groups	# Misplaced Vars	Grouping Accuracy
LSMOP1	0/0/0	0/0/0	0/0/0	−/−/−
LSMOP2	205/205/205	10/10/10	0/0/0	100.00%/100.00%/100.00%
LSMOP3	145/145/145	5/5/5	0/0/0	100.00%/100.00%/100.00%
LSMOP4	204/205/205	10/10/10	1/0/0	99.31%/100.00%/100.00%
LSMOP5	0/0/0	0/0/0	0/0/0	−/−/−
LSMOP6	205/205/205	10/10/10	0/0/0	100.00%/100.00%/100.00%
LSMOP7	145/205/205	5/10/10	0/0/0	100.00%/100.00%/100.00%
LSMOP8	59/60/60	5/5/5	1/0/0	98.33%/100.00%/100.00%
LSMOP9	145/145/145	5/5/5	0/0/0	−/−/−

Table 8
Variable Analysis Results Obtained Using mogDG-shift on 3-objective LSMOPs with $\omega = 10^{-4}/10^{-6}/10^{-8}, \gamma^I = 111.1$

Function	# Captured Non-sep Vars	# Formed Non-sep Groups	# Misplaced Vars	Grouping Accuracy
LSMOP1	0/0/0	0/0/0	0/0/0	−/−/−
LSMOP2	239/305/305	10/15/15	66/0/0	78.36%/100.00%/100.00%
LSMOP3	155/155/155	5/5/5	0/0/0	100.00%/100.00%/100.00%
LSMOP4	240/305/305	10/15/15	0/0/0	100.00%/100.00%/100.00%
LSMOP5	0/0/0	0/0/0	0/0/0	−/−/−
LSMOP6	150/305/305	10/15/15	155/0/0	49.18%/100.00%/100.00%
LSMOP7	240/305/305	10/15/15	0/0/0	100.00%/100.00%/100.00%
LSMOP8	150/150/150	10/10/10	0/0/0	100.00%/100.00%/100.00%
LSMOP9	155/155/155	5/5/5	0/0/0	−/−/−

Table 9
Variable Analysis Results of moDG2 and moDG2-shift on 2-objective LSMOPs with $\gamma^I = 11.1/111.1/1111.1$

Function	#Captured Non-sep Vars	#Formed Non-sep Groups	#Misplaced Vars	Grouping Accuracy
LSMOP1	0/22/78/101	0/**7**/**8**/**5**	0/0/0/0	−/−/−/−
LSMOP2	145/205/205/205	**5**/10/10/10	60/0/0/0	70.73%/100.00%/100.00%/100.00%
LSMOP3	145/147/163/160	**1**/**2**/**6**/**8**	0/0/0/0	100.00%/100.00%/100.00%/100.00%
LSMOP4	145/205/205/205	5/**10**/**10**/**10**	0/0/0/0	100.00%/100.00%/100.00%/100.00%
LSMOP5	0/115/126/127	0/**4**/**1**/**2**	0/0/0/0	−/−/−/−
LSMOP6	205/205/205/205	**8**/**2**/**7**/**4**	0/0/0/0	100.00%/100.00%/100.00%/100.00%
LSMOP7	205/205/205/205	**6**/**1**/**1**/**1**	0/0/0/0	100.00%/100.00%/100.00%/100.00%
LSMOP8	60/104/126/124	5/**8**/**6**/**6**	0/0/0/0	100.00%/100.00%/100.00%/100.00%
LSMOP9	145/145/164/161	**5**/**5**/**6**/**6**	0/0/0/0	−/−/−/−

Table 10
Variable Analysis Results of moDG2 and moDG2-shift on 3-objective LSMOPs with $\gamma^I = 11.1/111.1/1111.1$

Function	#Captured Non-sep Vars	#Formed Non-sep Groups	#Misplaced Vars	Grouping Accuracy
LSMOP1	4/47/105/100	**2**/**9**/**10**/**9**	0/0/0/0	−/−/−/−
LSMOP2	85/305/305/305	**5**/**15**/**11**/**13**	220/0/0/0	27.87%/100.00%/100.00%/100.00%
LSMOP3	2/171/262/256	**1**/**6**/**5**/**5**	155/0/0/0	0.00%/100.00%/100.00%/100.00%
LSMOP4	85/305/305/305	**5**/**15**/**10**/**15**	155/0/0/0	0.00%/100.00%/100.00%/100.00%
LSMOP5	0/70/137/181	0/**13**/**9**/**10**	0/0/0/0	−/−/−/−
LSMOP6	220/305/305/305	**8**/**1**/**3**/**3**	85/0/0/0	72.13%/100.00%/100.00%/100.00%
LSMOP7	220/305/305/305	**6**/**1**/**2**/**1**	0/0/0/0	100.00%/100.00%/100.00%/100.00%
LSMOP8	65/245/204/235	**5**/**9**/**16**/**12**	85/0/0/0	43.33%/100.00%/100.00%/100.00%
LSMOP9	155/184/181/167	**5**/**2**/**7**/**8**	0/0/0/0	−/−/−/−

6.1. Parameter settings

To perform a fair comparison, we set the population size (*NP*) to 100 for the 2-objective test instances and to 105 for the 3-objective test instances for all of the algorithms as recommended in Ref. [26].

For *DE*, *F* and *CR* are set to 0.5 and 1.0, respectively. The neighborhood size and replacement limit for MOEA/D-DE and CCMOEA/D-DE are set to 20 and 2 [26], respectively, and the probability of selecting parents from the neighborhood is 0.9. The distribution index is 20.

As discussed in Section 5, in mogDG-shift and moDG2-shift, we set $\gamma^I = 111.1$ and $\omega = 10^{-6}$ for the 2-/3-objective test instances. The group size for separable variables is 30. Finally, N_{PA} is set to 20, and $\gamma^P = 111.1$.

According to Ref. [26], the number of FEs is set to $(nObj \times 1000 \times NP)$. Here, *nObj* is the number of objectives. For each test instance, the optimization is performed 30 times.

Table 11
Grouping Comparison of mogDG-shift, moDG2-shift and DVA on 2-/3-objective LSMOPs.

Function	#Captured Non-sep Vars	#Formed Non-sep Groups	#Misplaced Vars	Grouping Accuracy
LSMOP1	0/0	0/0	0/0	−/−
	45/104	9/13	0/0	−/−
	0/0	0/0	0/0	−/−
LSMOP2	205/305	10/15	0/0	100.00%/100.00%
	205/305	10/9	0/0	100.00%/100.00%
	60/150	5/10	145/155	29.27%/49.18%
LSMOP3	145/155	5/5	0/0	100.00%/100.00%
	147/165	2/5	0/0	100.00%/100.00%
	142.37/152.30	19.40/19.87	2.63/2.70	98.18%/98.26%
LSMOP4	205/305	10/15	0/0	100.00%/100.00%
	205/305	10/13	0/0	100.00%/100.00%
	190.80/287.70	13.40/19.20	0/0	100.00%/100.00%
LSMOP5	0/0	0/0	0/0	−/−
	127/192	1/6	0/0	−/−
	0/0	0/0	0/0	−/−
LSMOP6	205/305	10/15	0/0	100.00%/100.00%
	205/305	7/2	0/0	100.00%/100.00%
	56.23/143.57	13.30/27.17	148.77/161.43	27.43%/47.07%
LSMOP7	205/305	10/15	0/0	100.00%/100.00%
	205/305	1/2	0/0	100.00%/100.00%
	191.00/288.53	25.97/33.90	2.63/2.57	98.18%/98.34%
LSMOP8	60/150	5/10	0/0	100.00%/100.00%
	124/232	7/13	0/0	100.00%/100.00%
	60/150	5/10	0/0	100.00%/100.00%
LSMOP9	145/155	5/5	0/0	−/−
	149/194	7/3	0/0	−/−
	137.03/147.93	6.50/5.87	0/0	−/−

Table 12
FEs consumed by three grouping methods.

	gDG	DG2	DVA
FEs	21116/46666	21116/46666	380070/845478

Table 13
Average ranking of CCMOEA/D and CCNSGA-II with different group sizes (Friedman).

Algorithm	Ranking	Final Ranking
M-30	3.2222	1
M-50	3.3333	2
M-10	3.5000	3
M-∞	4.0000	4
M-1	4.3333	5
N-10	6.6111	6
N-30	6.8889	7
N-50	7.2222	8
N-1	7.6111	9
N-∞	8.2778	10

6.2. Optimization performance indicator and statistical analysis

The inverted generational distance (IGD) indicator [31] is employed for performance assessment. To calculate the IGD value I_{IGD}, let S_{POF} and S_{PF} denote the POF and the estimated PF; the following equation is formulated:

$$I_{IGD} = \frac{\sum_{p \in S_{POF}} d(p, S_{PF})}{|S_{POF}|} \tag{28}$$

where p is the element in S_{POF}, $d(p, S_{PF})$ is the Euclidean distance of p to its nearest element in S_{PF}, and $|S|$ denotes the cardinality of set S. A lower IGD value indicates better performance.

Because we have numerous test instances (nine problems each tested with two different objective numbers), we use a non-parametric test [28,29] to rank the algorithms.

6.3. Minor improvements

Similar to MOEA/DVA, to initialize the diversity-related variables, we can randomly or uniformly sample their values in the search space. The specific description is as follows:

1) Random Sampling: For each individual in the population, every variable randomly takes a value within its search range;
2) Uniform Sampling: All individuals are uniformly scattered in the whole search space, and in this hyperspace, the distance of each individual to its nearest neighboring individual is the same.

Table 14 shows the differences between uniform and random samplings of the diversity-related variables regarding the optimization performance, and the detailed optimization results are listed in

Table 14
Average ranking for mean IGD values (Friedman).

Algorithm	Ranking	Final Ranking
CCMOEA/D-DE-u	1.6667	1
CCMOEA/D-DE-r	2.0000	2
CCNSGA–II–DE-u	3.0000	3
CCNSGA–II–DE-r	3.3333	4

Table 15
Average ranking for mean IGD values (Friedman).

Algorithm	Ranking	Final Ranking
CCMOEA/D-DE-g	1.3333	1
CCMOEA/D-DE-l	2.1667	2
CCNSGA–II–DE-g	3.2222	3
CCNSGA–II–DE-l	3.2778	4

Table 16
Mean values and standard deviations of IGD for MOEA/D-DE, NSGA–II–DE, CCMOEA/D-DE, CCNSGA–II–DE, CC2MOEA/D-DE and CC2NSGA–II–DE

IGD	MOEA/D-DE		NSGA–II–DE		CCMOEA/D-DE		CCNSGA–II–DE		CC2MOEA/D-DE		CC2NSGA–II–DE	
2obj_LSMOP2	0.086097	(0.002363)	0.090814	**(0.001489)**	**0.068853**	(0.002341)	0.076427	(0.004320)	**0.068853**	(0.002341)	0.076427	(0.004320)
2obj_LSMOP3	**0.642353**	(0.082891)	11.667501	(5.396436)	0.707755	**(0.000197)**	2.686907	(0.586555)	0.700961	(0.036958)	5.472856	(2.277113)
2obj_LSMOP4	0.037210	(0.011903)	**0.027718**	**(0.001583)**	0.077653	(0.003966)	0.100774	(0.002392)	0.077653	(0.003966)	0.100774	(0.002392)
2obj_LSMOP5	**0.010947**	**(0.000962)**	0.577275	(0.254336)	0.247348	(0.083495)	0.324025	(0.031075)	0.342186	(0.008541)	0.616267	(0.174262)
2obj_LSMOP6	0.718833	(0.067268)	0.638798	(0.139302)	0.752859	**(0.001926)**	**0.466614**	(0.010166)	0.749756	(0.002390)	0.516248	(0.086492)
2obj_LSMOP7	**1.819453**	**(0.333994)**	7.711964	(4.453682)	2.229473	(0.513449)	2.760915	(0.633064)	2.198360	(0.400588)	4.735421	(0.963376)
2obj_LSMOP8	**0.048654**	(0.002712)	0.091838	(0.007913)	0.165085	(0.006740)	0.344828	**(0.001813)**	0.177949	(0.040351)	0.344399	(0.001828)
2obj_LSMOP9	**0.353425**	**(0.012763)**	1.592608	(0.351631)	0.506980	(0.021936)	0.986034	(0.392932)	0.505689	(0.022139)	1.205067	(0.356838)
3obj_LSMOP1	1.151486	(0.107965)	1.380947	(0.469479)	**0.242852**	**(0.019790)**	0.927520	(0.299078)	0.260610	(0.036555)	1.455198	(0.406376)
3obj_LSMOP2	0.081910	(0.001168)	0.101876	(0.001910)	0.074757	**(0.000636)**	0.089817	(0.002085)	**0.074691**	(0.000810)	0.090048	(0.002239)
3obj_LSMOP3	8.015751	(0.927778)	29.746629	(8.064804)	0.922199	(0.302548)	11.604761	(1.955795)	**0.836143**	**(0.036721)**	10.345528	(1.516117)
3obj_LSMOP4	0.217986	**(0.002826)**	0.276705	(0.008500)	0.160042	(0.005774)	0.212207	(0.004839)	**0.154798**	(0.006451)	0.213910	(0.004783)
3obj_LSMOP5	0.914140	(0.293686)	2.047144	(0.904207)	**0.350113**	**(0.022908)**	0.420065	(0.035033)	0.398951	(0.065685)	2.899935	(0.617580)
3obj_LSMOP6	**1.429093**	(0.445785)	11.437091	(12.028125)	1.505527	**(0.283009)**	2.484714	(1.025952)	1.549150	(0.402319)	313.920683	(873.757438)
3obj_LSMOP7	**0.836083**	(0.164532)	1.531751	(0.092844)	0.946167	(0.000041)	1.174111	(0.129264)	0.946063	**(0.000025)**	1.432856	(0.094275)
3obj_LSMOP8	0.556206	**(0.016087)**	0.261170	(0.027774)	0.353804	(0.023434)	**0.254889**	(0.008567)	0.339823	(0.041969)	0.260941	(0.019589)
3obj_LSMOP9	**0.508281**	**(0.068574)**	3.563485	(1.017774)	0.752386	(0.328042)	1.808434	(0.344790)	1.004374	(0.406826)	2.517812	(0.454503)

Note 1: Values in parentheses are standard deviations.
Note 2: Values in bold denote better performances.

the supplementary material. Other parameters are set as mentioned above.

From the rankings of the algorithms, the difference is small, but the uniform sampling seems slightly better. We can infer that, compared to random sampling, individuals are uniformly scattered in the search space when performing uniform sampling, and thus the corresponding search space can be more thoroughly explored. Therefore, in this paper, we employ uniform sampling to initialize the diversity-related variables.

In the experiments, after the evolution of a variable group, the scope of performing *realmutation* could exert some influence on the optimization performance. Two kinds of methods are used in experiments:

1) performing *realmutation* on the evolved variables within the group;
2) performing *realmutation* on the entire combined solution vector.

Table 15 demonstrates the ranking results by adopting the above two mutation strategies, while the detailed optimization results are listed in the supplementary material. The probabilities of *realmutation* are $1/nVar$ and $1/nDim$, respectively, where *nVar* is the number of variables in the current group, and *nDim* is the number of variables, while the other parameters are set as described above. As listed in Table 15, mutation method 2 is quite beneficial for the CCMOEA/D-DE algorithm, while for the CCNSGA–II–DE algorithm, method 2 is slightly better. Therefore, for *polynomial mutation*, we use method 2 and set the mutation probability to $1.0/nDim$.

6.4. Experimental results

The comparisons of the IGD indicator are listed in Table 16. As shown by the IGD values in Table 16, for the 2-objective problems, MOEA/D-DE performs the best on 5 of the 9 instances, while for the 3-objective problems, CCMOEA/D-DE performs the best on 3 of the 9 instances. The rankings of all algorithms are listed in Table 17. For the IGD indicator, the performance of NSGA–II–DE improves when mogDG-shift or moDG2-shift is utilized; when compared to MOEA/D-DE, the optimization results of the CC algorithms are quite similar.

We also rank the algorithms for the 2-/3-objective instances, respectively (see Tables 18 and 19). For the 2-objective instances, CCNSGA–II–DE performs better than NSGA–II–DE; for MOEA/D-DE, the CC framework is not beneficial. However, for the 3-objective instances, MOEA/D-DE and NSGA–II–DE are both much improved. As there are more groups and variables in the 3-objective instances than in the 2-objective instances, the contributions of mogDG-shift and moDG2-shift are more beneficial.

The FEs used for mogDG-shift and moDG2-shift comprise approximately 12.62% and 16.76% of the allowed FEs for the 2-/3-objective instances, respectively. Therefore, we can infer that, although the variable grouping consumes a substantial portion of the FEs, the optimization performance is improved due to accurate recognition and grouping of the non-separable variables.

In Table 20, we list the time consumed by all six algorithms for each test problem and their sums. According to the table, we can see that compared to the original algorithms, the corresponding CC-based ones take less time for NSGA–II–DE but are comparable for MOEA/D-DE.

7. Additional experiments on other test suites

To further validate the proposed grouping method and improvement strategies, we also compare the aforementioned six algorithms with respect to additional multiobjective test suites: DTLZ [24] and WFG [15]. Corresponding to LSMOP, the objective numbers are 2 and 3, and the numbers of variables are 200 and 300, respectively. The same parameter settings described in the prior section are adopted here.

Table 17
Average ranking of MOEA/D-DE, NSGA–II–DE, CCMOEA/D-DE, CCNSGA–II–DE, CC2MOEA/D-DE and CC2NSGA–II–DE (Friedman).

Algorithm	Ranking	Final Ranking
MOEA/D-DE	2.5000	1
CCMOEA/D-DE	2.6111	2
CC2MOEA/D-DE	2.6111	3
CCNSGA–II–DE	3.6111	4
CC2NSGA–II–DE	4.7222	5
NSGA–II–DE	4.9444	6

Table 18
Average ranking of MOEA/D-DE, NSGA–II–DE, CCMOEA/D-DE, CCNSGA–II–DE, CC2MOEA/D-DE and CC2NSGA–II–DE (Friedman).

Algorithm	Ranking	Final Ranking
MOEA/D-DE	1.8889	1
CCMOEA/D-DE	3.0000	2
CC2MOEA/D-DE	3.1111	3
CCNSGA–II–DE	3.7778	4
NSGA–II–DE	4.5556	5
CC2NSGA–II–DE	4.6667	6

Note: Mean IGD values for the 2-objective instances.

Table 19
Average ranking of MOEA/D-DE, NSGA–II–DE, CCMOEA/D-DE, CCNSGA–II–DE, CC2MOEA/D-DE and CC2NSGA–II–DE (Friedman).

Algorithm	Ranking	Final Ranking
CC2MOEA/D-DE	2.1111	1
CCMOEA/D-DE	2.2222	2
MOEA/D-DE	3.1111	3
CCNSGA–II–DE	3.4444	4
CC2NSGA–II–DE	4.7778	5
NSGA–II–DE	5.3333	6

Note: Mean IGD values for the 3-objective instances.

7.1. Variable analysis

As to the groundtruth, the number of diversity-related variables for DTLZ is $(nObj - 1)$; for WFG, as the position-related parameter is set as $k = 2(nObj - 1)$, there exist $2(nObj - 1)$ diversity-related variables.

For Algorithm 1, with N_{PA} fixed to 20, we examine different γ^I values of 11.1, 111.1 and 1111.1, as well as no added shifts corresponding to replacing Line 7 in Algorithm 1 with the following:

$$\boldsymbol{Y}_k = \frac{(j - 0.5)}{N_{PA}} \times \left(\boldsymbol{X}_k^u - \boldsymbol{X}_k^l\right) + \boldsymbol{X}_k^l \tag{29}$$

and Line 9 with:

$$\boldsymbol{Y}_k = 0.5 \times \left(\boldsymbol{X}_k^l + \boldsymbol{X}_k^u\right) \tag{30}$$

For all four cases, in WFG7 and WFG9, there exist dependencies of each variable on the subsequent ones. The first $2(nObj - 1)$ variables are diversity variables, and thus each variable influences the true diversity variables. As a result, Algorithm 1 identifies almost all variables as diversity-related variables. For DTLZ, Algorithm 1 without shift cannot recognize all diversity-related variables for 3-objective DTLZ5, while for γ^I with 3 different settings, the tests are passed for all instances. Thus, we simply set $\gamma^I = 111.1$.

For DVA, the situation is similar for WFG7 and WFG9. In addition, for 3-objective WFG3, although all true diversity variables are recognized, few other variables are also included. For DTLZ, the tests are passed for all 30 runs.

7.2. Variable grouping

The interaction pattern of DTLZ and WFG can be summarized as follows:

- Fully separable: DTLZ 1–7, WFG1, WFG4-5, and WFG7.
- Fully non-separable: WFG6 and WFG8-9.
- Partially non-separable: WFG2-3. The groundtruth is listed in Table 21, in which each non-separable group contains 2 variables.

Correspondingly, we provide the grouping results as follows:

- Fully separable: All algorithms fail for WFG7. For the remaining ones, mogDG-shift and DVA recognize all variables as separa-

Table 21
Grouping groundtruth of 2-/3-objective WFG2-3.

Function	Sep Vars	Non-sep Vars	Non-sep Groups
WFG2	0/0	198/296	99/148
WFG3	0/0	198/296	99/148

Table 20
Time consumptions for MOEA/D-DE, NSGA–II–DE, CCMOEA/D-DE, CCNSGA–II–DE, CC2MOEA/D-DE and CC2NSGA–II–DE

	MOEA/D-DE	NSGA–II–DE	CCMOEA/D-DE	CCNSGA–II–DE	CC2MOEA/D-DE	CC2NSGA–II–DE
2obj_LSMOP1	2.225993	3.790790	2.298359	3.417804	2.190812	3.310195
2obj_LSMOP2	2.411246	3.976330	2.449400	3.584822	2.434788	3.576144
2obj_LSMOP3	2.313157	3.800802	2.421736	3.522697	2.375635	3.476145
2obj_LSMOP4	2.791520	4.399815	2.848987	4.028355	2.801205	3.977458
2obj_LSMOP5	2.603605	4.313243	2.693323	3.844788	2.846002	3.971587
2obj_LSMOP6	2.567495	4.077373	2.614959	3.708768	2.654038	3.757195
2obj_LSMOP7	2.738022	4.245360	2.813589	3.910788	3.250268	4.507430
2obj_LSMOP8	2.810076	4.315305	2.816311	3.921188	2.805851	3.902529
2obj_LSMOP9	3.106724	4.631347	3.072607	4.171250	3.013024	4.116003
3obj_LSMOP1	5.007556	8.801483	5.051088	7.550085	4.755426	7.285453
3obj_LSMOP2	5.863965	10.357599	5.641222	8.073820	5.722529	8.169554
3obj_LSMOP3	5.562038	9.038368	5.644370	8.014474	5.731093	8.199624
3obj_LSMOP4	6.368075	10.931907	6.261954	8.837100	6.262634	8.850911
3obj_LSMOP5	5.939410	10.244310	6.122882	8.676234	5.723296	8.236956
3obj_LSMOP6	5.874055	10.032058	5.882973	8.299065	6.743706	9.195374
3obj_LSMOP7	6.401684	10.353771	6.504705	8.947012	7.347441	10.097414
3obj_LSMOP8	6.662324	10.913820	6.608378	9.045530	6.309988	8.703770
3obj_LSMOP9	6.490527	10.586748	6.713018	9.045250	6.305247	8.658980
SUM	77.737470	128.810430	78.459861	110.599032	79.272981	111.992723

Note: The unit is seconds.

Table 22
IGD mean values and standard deviations of MOEA/D-DE, NSGA–II–DE, CCMOEA/D-DE, CCNSGA–II–DE, CC2MOEA/D-DE and CC2NSGA–II–DE for DTLZ and WFG.

IGD	MOEA/D-DE		NSGA–II–DE		CCMOEA/D-DE		CCNSGA–II–DE		CC2MOEA/D-DE		CC2NSGA–II–DE	
2obj_DTLZ1	400.097732	(354.289464)	**10.781767**	**(25.797099)**	684.859843	(132.016691)	895.056103	(88.315468)	684.859843	(132.016691)	895.056103	(88.315468)
2obj_DTLZ2	0.008367	(0.000446)	0.177871	(0.086266)	**0.004981**	**(0.000095)**	0.009842	(0.000522)	**0.004981**	**(0.000095)**	0.009842	(0.000522)
2obj_DTLZ3	1379.658790	(1259.281394)	**18.795674**	**(37.940504)**	1848.928858	(398.221621)	2320.725020	(225.315103)	1848.928858	(398.221621)	2320.725020	(225.315103)
2obj_DTLZ4	0.136980	(0.270840)	0.047480	(0.129039)	0.226163	(0.337764)	**0.009450**	**(0.000630)**	0.226163	(0.337764)	**0.009450**	**(0.000630)**
2obj_DTLZ5	0.008367	(0.000446)	0.175912	(0.086630)	**0.004981**	**(0.000095)**	0.010037	(0.000851)	**0.004981**	**(0.000095)**	0.010037	(0.000851)
2obj_DTLZ6	**0.004722**	**(0.000235)**	37.620835	(7.250123)	7.772043	(1.754552)	51.785732	(4.379724)	7.772043	(1.754552)	51.785732	(4.379724)
2obj_DTLZ7	0.063140	(0.129879)	0.670400	(0.257200)	**0.008546**	**(0.000375)**	0.082007	(0.032189)	**0.008546**	**(0.000375)**	0.082007	(0.032189)
3obj_DTLZ1	**386.358537**	(348.694018)	913.173395	(1128.032679)	955.643273	**(139.803388)**	3308.127678	(182.562245)	955.643273	**(139.803388)**	3308.127678	(182.562245)
3obj_DTLZ2	0.250181	(0.028759)	3.413273	(1.240964)	**0.069198**	**(0.000436)**	0.146414	(0.010569)	**0.069198**	**(0.000436)**	0.146414	(0.010569)
3obj_DTLZ3	471.403202	(642.326534)	**265.423110**	**(305.991961)**	3097.451460	(465.480944)	8254.128480	(450.783024)	3638.998384	(564.940204)	8362.816398	(759.734868)
3obj_DTLZ4	0.430542	(0.154607)	0.547460	(0.118037)	**0.078549**	(0.033727)	0.113318	**(0.007113)**	**0.078549**	(0.033727)	0.113318	**(0.007113)**
3obj_DTLZ5	0.093283	(0.010473)	2.369993	(0.985241)	**0.012780**	**(0.000139)**	0.039212	(0.003022)	0.013838	(0.000280)	0.054678	(0.009476)
3obj_DTLZ6	**0.012523**	**(0.000193)**	142.688845	(6.966044)	4.997141	(2.263068)	148.826140	(3.787227)	0.012792	(0.000559)	130.228322	(16.778498)
3obj_DTLZ7	0.988598	(0.139306)	5.878451	(0.425870)	**0.176005**	**(0.013711)**	0.786948	(0.107808)	**0.176005**	**(0.013711)**	0.786948	(0.107808)
2obj_WFG1	1.265178	(0.003552)	1.277764	**(0.003089)**	1.218480	(0.006503)	1.238028	(0.004196)	**1.213142**	(0.007368)	1.237302	(0.004593)
2obj_WFG2	0.136696	(0.013093)	0.155674	(0.014610)	0.126445	(0.088858)	**0.064313**	**(0.004164)**	0.126445	(0.088858)	**0.064313**	**(0.004164)**
2obj_WFG3	0.159832	(0.006816)	0.151928	(0.008594)	**0.065484**	(0.006516)	0.102859	**(0.006263)**	**0.065484**	(0.006516)	0.102859	**(0.006263)**
2obj_WFG4	0.139472	(0.006939)	0.144168	**(0.003363)**	**0.058725**	(0.004030)	0.080077	(0.004503)	**0.058725**	(0.004030)	0.080077	(0.004503)
2obj_WFG5	0.072005	(0.000719)	0.076192	(0.001706)	**0.070695**	**(0.000209)**	0.078156	(0.001711)	**0.070695**	**(0.000209)**	0.078156	(0.001711)
2obj_WFG6	**0.021464**	**(0.000950)**	0.055651	(0.036377)	0.023084	(0.001886)	0.045116	(0.002091)	0.023084	(0.001886)	0.045116	(0.002091)
2obj_WFG7	**0.041069**	**(0.002740)**	0.102484	(0.007644)	0.041789	(0.002880)	0.104330	(0.007807)	0.041789	(0.002880)	0.104330	(0.007807)
2obj_WFG8	0.168176	(0.009678)	0.190981	(0.012979)	**0.166862**	(0.013603)	0.211112	**(0.009380)**	**0.166862**	(0.013603)	0.211112	**(0.009380)**
2obj_WFG9	**0.031616**	(0.017566)	0.081780	(0.011672)	0.031696	(0.017714)	0.082787	**(0.011606)**	0.031696	(0.017714)	0.082787	**(0.011606)**
3obj_WFG1	1.554247	**(0.004296)**	1.621632	(0.040689)	**1.490375**	(0.010293)	1.588323	(0.054779)	1.494135	(0.009108)	1.580353	(0.040872)
3obj_WFG2	0.623931	**(0.010804)**	0.433477	(0.013067)	0.559029	(0.015823)	**0.284860**	(0.011784)	0.559029	(0.015823)	**0.284860**	(0.011784)
3obj_WFG3	0.441204	(0.013016)	0.468724	(0.020787)	**0.125112**	**(0.006729)**	0.258720	(0.012010)	**0.125112**	**(0.006729)**	0.258720	(0.012010)
3obj_WFG4	0.415030	(0.010882)	0.506152	(0.018180)	0.342661	**(0.004252)**	**0.296492**	(0.007068)	0.342661	**(0.004252)**	**0.296492**	(0.007068)
3obj_WFG5	0.317982	**(0.001757)**	0.327892	(0.027003)	0.311986	(0.002255)	0.268231	(0.008218)	0.312156	(0.002632)	**0.265617**	(0.009468)
3obj_WFG6	0.325218	(0.002191)	**0.297733**	(0.019601)	0.327593	**(0.001806)**	0.317868	(0.021155)	0.327593	**(0.001806)**	0.317868	(0.021155)
3obj_WFG7	**0.433006**	(0.010608)	0.609142	(0.024248)	0.433556	**(0.010493)**	0.611296	(0.027623)	0.433556	**(0.010493)**	0.611296	(0.027623)
3obj_WFG8	0.484037	(0.012464)	0.640040	(0.018149)	**0.382711**	**(0.007132)**	0.414314	(0.012515)	**0.382711**	**(0.007132)**	0.414314	(0.012515)
3obj_WFG9	**0.308159**	(0.013132)	0.443460	(0.044990)	0.308320	**(0.013123)**	0.445648	(0.047060)	0.308320	**(0.013123)**	0.445648	(0.047060)

Note 1: Values in parentheses are standard deviations.
Note 2: Values in bold denote better performances.

Table 23
Average ranking of MOEA/D-DE, NSGA–II–DE, CCMOEA/D-DE, CCNSGA–II–DE, CC2MOEA/D-DE and CC2NSGA–II–DE (Friedman) for DTLZ and WFG.

Algorithm	Ranking	Final Ranking
CCMOEA/D-DE	2.4688	1
CC2MOEA/D-DE	2.5312	2
MOEA/D-DE	3.3438	3
CC2NSGA–II–DE	4.0000	4
CCNSGA–II–DE	4.0938	5
NSGA–II–DE	4.5625	6

ble; moDG2-shift incorrectly forms non-separable groups for some instances;

- Fully non-separable: All algorithms fail for WFG9. For WFG6 and WFG8, mogDG-shift and moDG2-shift have both passed the tests; DVA is not stable and can miss few variables.
- Partially non-separable: For all instances, mogDG-shift and moDG2-shift have succeeded; some variables are unrecognized for DVA and not all groups can be formed.

For detailed results, please refer the supplementary material.

7.3. Optimization results

Table 22 lists the mean IGD values and the corresponding standard deviations of all algorithms with respect to 2-/3-objective DTLZ and WFG instances. We can identify CCMOEA/D-DE as the best-performing, in accordance with the ranking results listed in Table 23. Compared to LSMOP, the CC framework is beneficial for both MOEA/D-DE and NSGA–II–DE with respect to 2-/3-objective instances.

The time consumed for DTLZ and WFG is listed in Table 24. There is no significant advantage for CC-based ones, but MOEA/D-DE and its CC-based ones are more efficient than the NSGA–II–DE algorithms.

8. Conclusion

This paper proposes the mogDG-shift method to decompose the large number of variables in MOLSOPs. For the 2-/3-objective test instances in the LSMOP test suite, mogDG-shift is able to detect all non-separable variables and correctly form corresponding non-separable groups. To examine the contribution of mogDG-shift to the optimization performance, we combine mogDG-shift with NSGA–II–DE and MOEA/D-DE (denoted as CCNSGA–II–DE and CCMOEA/D-DE, respectively). The results of experiments show that applying mogDG-shift to decompose the variables contributes to improved optimization performance. Additionally, for 2-/3-objective DTLZ and WFG, mogDG-shift can correctly recognize the variable properties, analyze the interdependences among variables and generate all non-separable groups for almost all test instances except WFG7 and WFG9. Further, the optimization performance improvement by utilizing the CC framework is much more significant compared to that on LSMOP. All in all, the proposed mogDG-shift is perfect for variable analysis and grouping, and further combined with CC-framework and other techniques, the optimization performance can be improved, though at the expense of a nontrivial amount of FEs.

Table 24
Time consumptions of MOEA/D-DE, NSGA–II–DE, CCMOEA/D-DE, CCNSGA–II–DE, CC2MOEA/D-DE and CC2NSGA–II–DE for DTLZ and WFG.

	MOEA/D-DE	NSGA–II–DE	CCMOEA/D-DE	CCNSGA–II–DE	CC2MOEA/D-DE	CC2NSGA–II–DE
2obj_DTLZ1	2.526371	4.054642	2.647558	3.674627	2.640139	3.662431
2obj_DTLZ2	2.058422	3.454301	2.188336	3.200473	2.196965	3.227310
2obj_DTLZ3	2.450260	3.919651	2.564757	3.634544	2.547276	3.602611
2obj_DTLZ4	2.055990	3.413022	2.168296	3.221820	2.180871	3.240976
2obj_DTLZ5	2.065319	3.448201	2.165021	3.200804	2.185292	3.220857
2obj_DTLZ6	3.939318	5.914177	3.873777	4.842627	4.165249	4.251377
2obj_DTLZ7	2.153165	3.803039	2.173934	3.242872	2.182639	3.264551
3obj_DTLZ1	5.673491	9.508442	5.745172	7.910606	5.667883	7.835458
3obj_DTLZ2	4.620518	8.015305	4.793038	6.993326	4.814907	7.012623
3obj_DTLZ3	5.577386	9.247573	5.793993	7.990947	5.826402	8.040243
3obj_DTLZ4	4.663839	7.788622	4.837271	7.043178	4.860925	7.070095
3obj_DTLZ5	4.647328	7.859200	4.822668	6.983010	6.310541	8.749897
3obj_DTLZ6	7.665667	11.087342	7.452541	9.646409	8.889945	11.406894
3obj_DTLZ7	5.034354	8.861340	4.795093	7.132790	4.817196	7.153105
2obj_WFG1	5.533690	7.165228	5.922540	7.051331	5.622783	6.722683
2obj_WFG2	3.572833	5.070575	3.533945	4.600219	3.466528	4.467514
2obj_WFG3	3.571564	5.107215	3.557115	4.611036	3.450229	4.489040
2obj_WFG4	4.344708	5.768191	4.719127	5.753667	4.448606	5.549596
2obj_WFG5	3.786908	5.492724	3.917419	5.034174	3.793802	4.904008
2obj_WFG6	33.509787	34.944628	36.910988	38.099802	33.849280	35.034352
2obj_WFG7	3.430276	4.955261	4.965150	6.485977	4.967721	6.571395
2obj_WFG8	15.781707	17.257399	17.625473	18.839038	16.306705	17.527192
2obj_WFG9	47.662660	48.872757	49.190523	50.442595	49.185467	50.526895
3obj_WFG1	13.130063	16.886078	13.824863	16.147621	12.781945	15.043118
3obj_WFG2	8.361900	11.086489	7.891004	9.999034	7.899979	9.555543
3obj_WFG3	8.247750	11.725044	7.996621	10.594392	7.569791	10.179563
3obj_WFG4	9.928468	13.778949	10.732472	13.083794	10.042295	12.400055
3obj_WFG5	9.100349	12.557819	8.970038	11.335037	9.167227	11.573747
3obj_WFG6	114.569191	117.634421	130.382272	132.755471	115.246582	117.692991
3obj_WFG7	8.228898	11.940887	13.243101	16.880905	13.199051	16.894062
3obj_WFG8	49.007959	52.752534	58.086859	59.593490	50.582397	53.228909
3obj_WFG9	159.637322	162.526060	164.739846	167.557123	164.687418	167.451504
SUM	556.537461	635.897118	602.230810	657.582738	575.554035	631.550596

Note: The unit is seconds.

Acknowledgements

This work was supported in part by the National Natural Science Foundation of China (NSFC) under Grants Nos. 61976242 and 61379060, in part by the by the Opening Project of Guangdong Province Key Laboratory of Computational Science at the Sun Yat-sen University under Grant No. 2018002, in part by the Foundation of Key Laboratory of Machine Intelligence and Advanced Computing of the Ministry of Education under Grant No. MSC-201602A, and in part by the Special Program for Applied Research on Super Computation of the NSFC-Guangdong Joint Fund (the second phase). This work is also supported in part by the National Supercomputer Center in Guangzhou and the National Supercomputer Center in Changsha.

Appendix A. Supplementary data

Supplementary data to this article can be found online at https://doi.org/10.1016/j.swevo.2019.100626.

References

[1] H. Seada, K. Deb, A unified evolutionary optimization procedure for single, multiple, and many objectives, IEEE Trans. Evol. Comput. 20 (3) (2016) 358–369.
[2] X. Ma, Q. Zhang, J. Yang, Z. Zhu, On Tchebycheff decomposition approaches for multi-objective evolutionary optimization, IEEE Trans. Evol. Comput. 22 (2) (2018) 226–244.
[3] A. Ponsich, A.L. Jaimes, C.A.C. Coello, A survey on multiobjective evolutionary algorithms for the solution of the portfolio optimization problem and other finance and economics applications, IEEE Trans. Evol. Comput. 17 (3) (2013) 321–344.
[4] J. Wang, Y. Cai, Multiobjective evolutionary algorithm for frequency assignment problem in satellite communications, Soft Computing 19 (5) (2015) 1229–1253.
[5] J. Branke, S. Nguyen, C.W. Pickardt, M. Zhang, Automated design of production scheduling heuristics: a review, IEEE Trans. Evol. Comput. 20 (1) (2016) 110–124.
[6] M. Tayaraninajaran, X. Yao, H. Xu, Meta-heuristic algorithms in car engine design: a literature survey, IEEE Trans. Evol. Comput. 19 (5) (2015) 609–629.
[7] A. Mukhopadhyay, U. Maulik, S. Bandyopadhyay, C.A.C. Coello, A survey of multiobjective evolutionary algorithms for data mining: Part I, IEEE Trans. Evol. Comput. 18 (1) (2014) 4–19.
[8] A. Mukhopadhyay, U. Maulik, S. Bandyopadhyay, C.A.C. Coello, Survey of multiobjective evolutionary algorithms for data mining: Part II, IEEE Trans. Evol. Comput. 18 (1) (2014) 20–35.
[9] Y. Zuo, M. Gong, J. Zeng, L. Ma, Personalized recommendation based on evolutionary multi-objective optimization [research frontier], IEEE Comput. Intell. Mag. 10 (1) (2015) 52–62.
[10] Q. Zhang, H. Li, MOEA/D: a multiobjective evolutionary algorithm based on decomposition, IEEE Trans. Evol. Comput. 11 (6) (2007) 712–731.
[11] K. Deb, A. Pratap, S. Agarwal, T. Meyarivan, A fast and elitist multiobjective genetic algorithm: nsga-II, IEEE Trans. Evol. Comput. 6 (2) (2002) 182–197.
[12] M.A. Potter, K.A. de Jong, A cooperative coevolutionary approach to function optimization, in: Parallel Problem Solving from Nature - PPSN III, vol. 886, 1994, pp. 249–257.
[13] M.A. Potter, K.A. de Jong, Cooperative coevolution: an architecture for evolving coadapted subcomponents, Evol. Comput. 8 (1) (2000) 1–29.
[14] Y. Ling, H. Li, B. Cao, Cooperative co-evolution with graph-based differential grouping for large scale global optimization, in: Proc. 2016 12th International Conference on Natural Computation, Fuzzy Systems and Knowledge Discovery, ICNCFSKD), 2016, pp. 1097–1104.
[15] S. Huband, P. Hingston, L. Barone, L. While, A review of multiobjective test problems and a scalable test problem toolkit, IEEE Trans. Evol. Comput. 10 (5) (2006) 477–506.
[16] X. Ma, et al., A multi-objective evolutionary algorithm based on decision variable analyses for multi-objective optimization problems with large-scale variables, IEEE Trans. Evol. Comput. 20 (2) (2016) 275–298.
[17] F. van den Bergh, A.P. Engelbrecht, A cooperative approach to particle swarm optimization 8 (3) (2004) 225–239.
[18] M.N. Omidvar, X. Li, X. Yao, Cooperative co-evolution with delta grouping for large-scale non-separable function optimization, in: Proc. IEEE Congr. Evol. Comput., 2010, pp. 1–8.
[19] X. Li, X. Yao, Cooperatively coevolving particle swarms for large-scale optimization, IEEE Trans. Evol. Comput. 16 (2) (2012) 210–224.
[20] M.N. Omidvar, X. Li, Y. Mei, X. Yao, Cooperative co-evolution with differential grouping for large-scale optimization, IEEE Trans. Evol. Comput. 18 (3) (2014) 378–393.
[21] Y. Mei, M.N. Omidvar, X. Li, X. Yao, A competitive divide-and-conquer algorithm for unconstrained large-scale black-box optimization, ACM Trans. Math Software 42 (2) (2016) 13:1–13:24.
[22] M.N. Omidvar, M. Yang, Y. Mei, X. Li, X. Yao, DG2: a faster and more accurate differential grouping for large-scale black-box optimization, IEEE Trans. Evol. Comput. 21 (6) (2017) 929–942.
[23] K. Tang, X. Yao, P. Suganthan, Benchmark functions for the CEC'2010 special session and competition on large scale global optimization, in: Proc. IEEE Congr. Evol. Comput., 2010, pp. 1–23.
[24] K. Deb, L. Thiele, M. Laumanns, E. Zitzler, Scalable multi-objective optimization test problems, in: Proceedings of the 2002 Congress on Evolutionary Computation, vol. 1, 2001, pp. 825–830.
[25] Q. Zhang, A. Zhou, S. Zhao, P.N. Suganthan, W. Liu, S. Tiwari, Multiobjective optimization test instances for the CEC 2009 special session and competition, in: Proc. IEEE Congr. Evol. Comput., 2009, pp. 1–30.
[26] R. Cheng, Y. Jin, M. Olhofer, B. Sendhoff, Test problems for large-scale multiobjective and many-objective optimization, IEEE Trans. Cybern. (2016) 1–14.
[27] X. Li, K. Tang, M.N. Omidvar, Z. Yang, K. Qin, Benchmark Functions for the CEC'2013 Special Session and Competition on Large-Scale Global Optimization, Tech. Rep., RMIT University, Melbourne, Australia, 2013. Tech. Rep..
[28] J. Derrac, S. García, D. Molina, F. Herrera, A practical tutorial on the use of nonparametric statistical tests as a methodology for comparing evolutionary and swarm intelligence algorithms, Swarm & Evol. Comput. 1 (1) (2011) 3–18.
[29] J. Alcalá-Fdez, et al., KEEL: a software tool to assess evolutionary algorithms to data mining problems, Soft Comput 13 (3) (2009) 307–318.
[30] H. Li, Q. Zhang, Multiobjective optimization problems with complicated Pareto sets, MOEA/D and NSGA-II, IEEE Trans. Evol. Comput. 13 (2) (2009) 284–302.
[31] E. Zitzler, L. Thiele, M. Laumanns, C.M. Fonseca, V.G. da Fonseca, Performance assessment of multiobjective optimizers: an analysis and review, IEEE Trans. Evol. Comput. 7 (2) (2003) 117–132.